2000 IEEE/EIA International Frequency Control Symposium and Exhibition

COMPARING PRIMARY FREQUENCY STANDARDS AT NIST AND PTB*

Lisa M. Nelson, NIST, Boulder, CO, USA
Judah Levine, NIST, Boulder, CO, USA
Peter Hetzel, PTB, Braunschweig, Germany

Abstract

We have constructed a link between the Physikalisch-Technische Bundesanstalt (PTB) in Braunschweig, Germany and the National Institute of Standards and Technology (NIST) in Boulder, Colorado using carrier-phase Global Positioning System (GPS) receivers. The link provides a direct measurement of the frequency difference between hydrogen maser H2(PTB) and UTC(NIST), and can also be used to provide a direct comparison between the primary frequency standards at the two laboratories. Based on our previous work with this method, we expect to be able to realize the frequency comparisons with an uncertainty of about 2×10^{-15} using several days of averaging. This uncertainty is smaller than the combined uncertainties of the primary frequency standards in both laboratories, and it therefore supports comparison of these primary frequency standards without degrading their capabilities with the noise of the transfer system.

Introduction

The goal of this experiment is to see how well we can compare atomic frequency standards between NIST and PTB using GPS carrier-phase data. We have previously analyzed this link using a few days of data. In this analysis we observe the standards for a few weeks. The techniques we used in this, and our previous analysis, are described in detail in [1]. The configurations at NIST and PTB are described below.

Figure 1 shows the NIST configuration. The GPS receiver and the Two-Way Satellite Time-Transfer (TWSTT) station are referenced to the Auxiliary Output Generator (AOG2) which is steered to UTC(NIST). The frequency estimated by the software analysis package described in [1-6] is combined with the measured frequency difference between AOG2, the maser and the primary frequency standards (NIST-7, NIST-F1) using data reported separately to the BIPM. The dotted lines indicate an evaluation of the maser frequency with respect to the corresponding primary frequency standard. The solid lines indicate direct electrical connections. AOG2 is under computer control and is digitally steered.

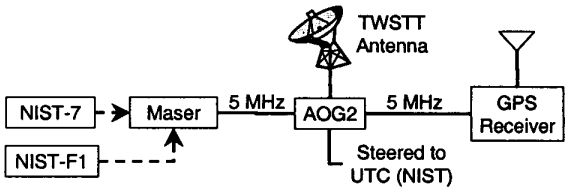

Figure 1: NIST Configuration Block Diagram.

The block diagram for the PTB configuration is shown in Figure 2. The GPS Receiver is referenced to hydrogen maser H2, which is the same reference used for PTB's TWSTT station. The dotted lines indicate that the maser frequency is compared to the primary frequency standard CS2 and to UTC(PTB). UTC(PTB) is directly derived from CS2 and steered to UTC(BIPM) by a micro-phase-stepper (MPS). To transform between H2 and UTC(PTB) or CS2 we use a smoothed hourly correction based on data provided by the PTB.

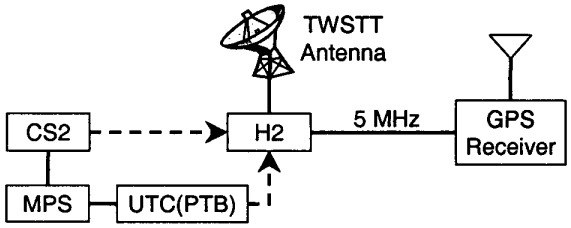

Figure 2: PTB Configuration Block Diagram.

Network Stations

To perform our measurement we use a network of geodetic-quality, dual-frequency GPS receivers. Some of the stations in the network come from International GPS Service (IGS) stations [7]. Figures 3 and 4 show the network station locations used in our analysis. In the analysis we use other nearby stations to help resolve carrier-phase cycle ambiguities.

The North American stations are shown in Figure 3. We have chosen a station 15 km northeast of NIST, TMGO, which has a rubidium reference clock. We also use ALGO, in Canada, to help define our reference frame, since its position is well known using very-long-baseline interferometry (VLBI). ALGO is 2290 km from NIST and 5860 km from PTB. The GPS receiver there is referenced to a hydrogen maser. NRC2, 199 km southeast of ALGO, was chosen to resolve ambiguities at

ALGO, and its receiver is also referenced to a hydrogen maser.

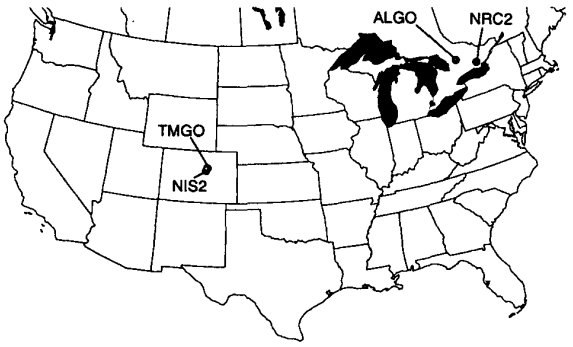

Figure 3: Network Stations in North America.

Figure 4 shows the station locations in Germany. In addition to PTB in Germany we use IGS stations POTS or WTZR. POTS is 178 km east of PTB and uses an internal oscillator as its reference. WTZR is 390 km southeast of PTB and has a hydrogen maser reference. We ran two different network solutions interchanging POTS and WTZR because of frequent data outages, and to see what effects this had on the clock estimate solution, specifically with the ambiguity resolution.

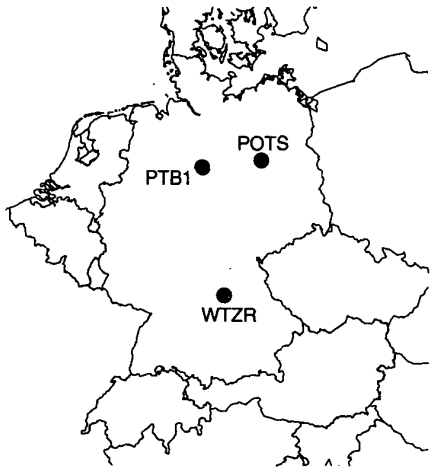

Figure 4: Network Stations in Germany.

Network Descriptions

For this paper we will use two different networks, which are described in Table 1. The main difference between the two different networks is that the second station used in Germany changes from WTZR to POTS.

Table 1: Network Names and Stations in each Network.

NETWORK NAME	STATIONS IN NETWORK
A	ALGO, NIST2, NRC2, PTB1, TMGO, WTZR
B	ALGO, NIST2, NRC2, POTS, PTB1, TMGO

Results

Figure 5 shows the 6-minute carrier phase clock estimates for H2(PTB) minus UTC(NIST) from MJD 51578-51626, approximately 48 days. Networks A and B have very similar results in the long term, which would lead us to believe that the selection of network stations, in general, is not critical. However, we are still experimenting with other locations with different reference clocks to confirm this. Reasons for this concern will be shown later in this paper.

The line with the diamond points is TWSTT data between H2(PTB) and UTC(NIST) over the same period, and the bias has been adjusted to see how well the carrier-phase and TWSTT results compare. In the short-term they follow each other closely. Even a rate change at MJD 51614, which is a real frequency change in H2, is seen similarly in the TWSTT and the carrier-phase data. However, we see a difference in the long-term comparison of the carrier-phase and TWSTT solutions.

Over this 48 d analysis period there is an accumulation of approximately 3 ns difference between the carrier-phase and TWSTT solutions. To determine the source of this difference we started by looking at where there were data outages. This is shown in Figure 5 with the vertical dashed lines appearing near the beginning of the analysis run and just after MJD 51614. These dashed lines represent data outages or jumps in network station data. The analysis of the handling of the outages did not produce conclusive results, so we looked into the way the data are combined to make the final solution.

For illustration, grid lines show the locations at which the various data were combined to produce the complete solution. Each solution was made on a 3.5 d interval with a half-day overlap with each adjacent solution. We are continuing our investigation into the contribution of data overlapping to the error budget and will show some of the initial results in the next section. Initial indications are that this may be the reason for the 3 ns difference in the carrier-phase and TWSTT solutions.

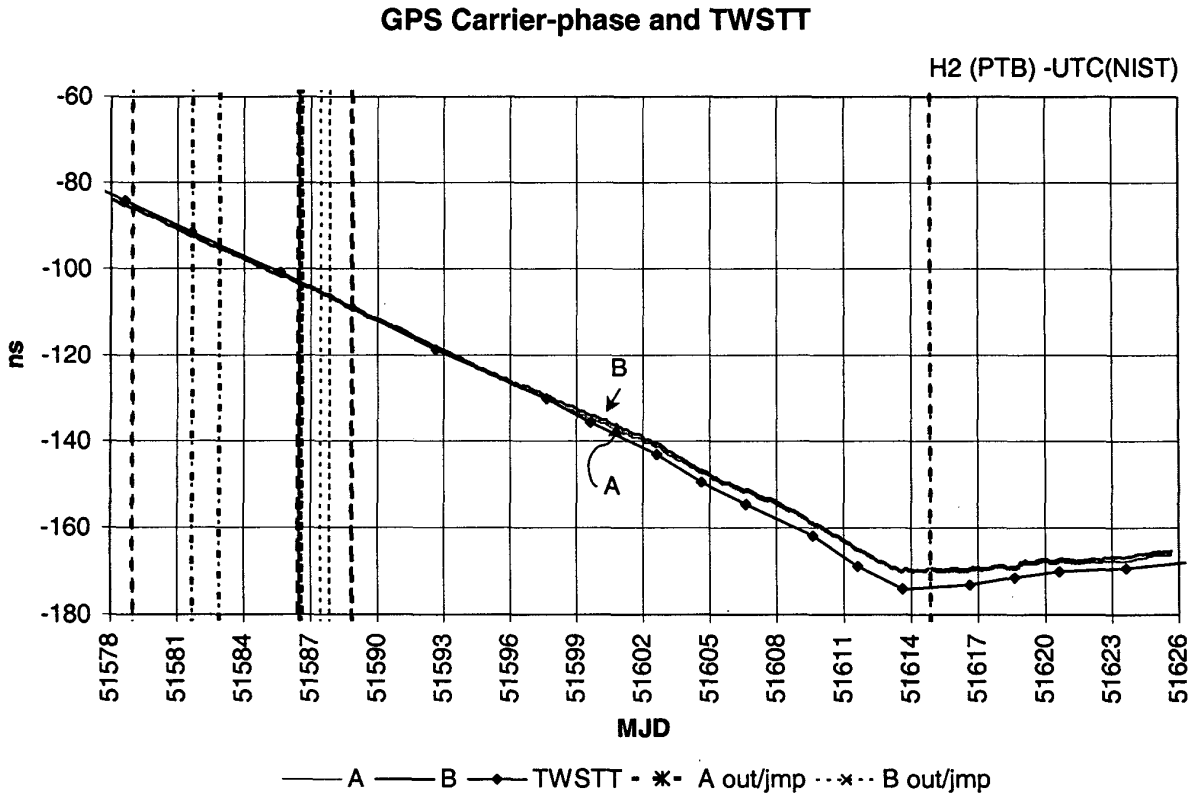

Figure 5: GPS Carrier-Phase and TWSTT data for H2(PTB) – UTC(NIST) from MJD 51578-51625.

Station Location Effects

Figure 6 is a plot of one 6.5 day portion of the data showing the solution for both networks as well as the TWSTT data. It is apparent that the carrier-phase solutions are very similar in the short term, but have a slight difference in rate.

A closer view of the data (Figure 7) shows a slight divergence in the two network solutions. To investigate the reason for this difference we have plotted differences between the bias-fixed and non-bias-fixed carrier-phase clock estimate solutions in Figures 8-11. Bias-fixed and non-bias-fixed solutions are the solutions with and without carrier-phase cycle ambiguity resolution, respectively.

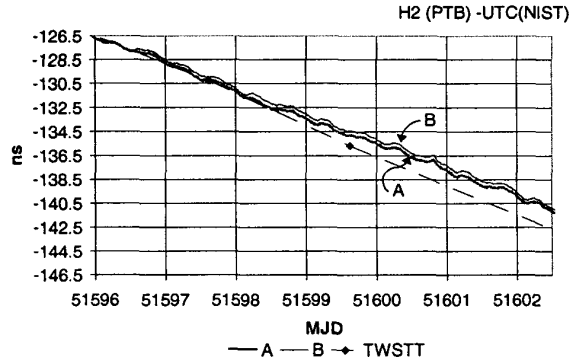

Figure 6: H2(PTB)-UTC(NIST) MJD 51596-51602.5 for Networks A, B and TWSTT.

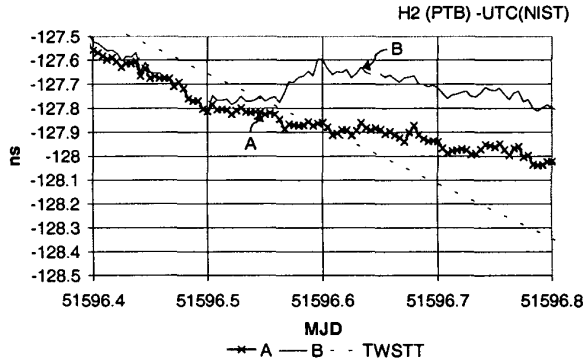

Figure 7: H2(PTB)-UTC(NIST) MJD 51596.4-51596.8 for Networks A, B and TWSTT.

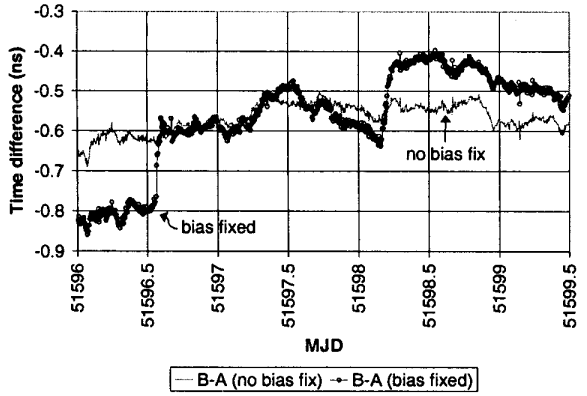

Figure 8: Differences between the two network solutions before and after bias fixing.

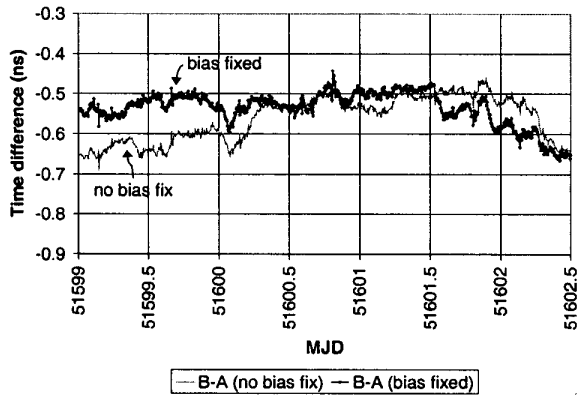

Figure 9: Differences between the two network solutions before and after bias fixing.

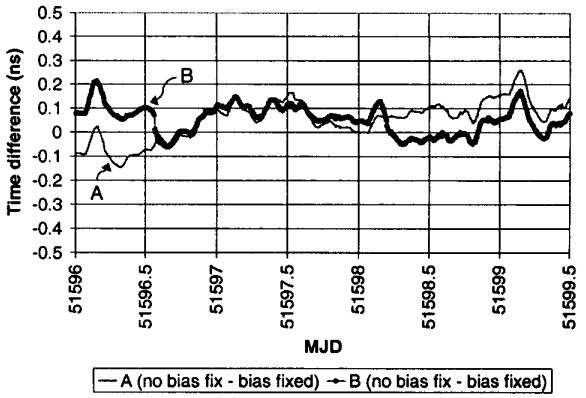

Figure 10: Differences between the bias-fixed and non-bias-fixed solutions for each network.

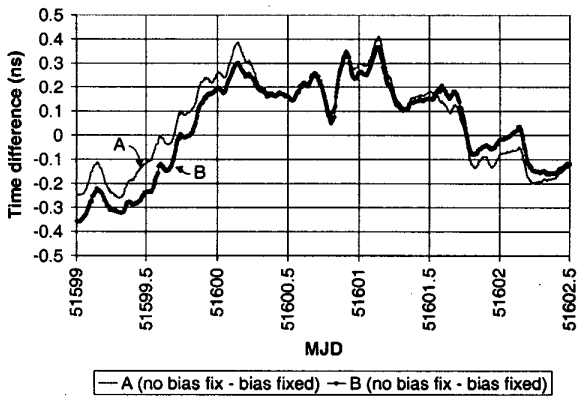

Figure 11: Differences between the bias-fixed and non-bias-fixed solutions for each network.

Figure 8 shows one 3.5-day data run where the difference in the two network solutions for the bias-fixed case spans 400 ps peak-to-peak and the non-bias-fixed solution is less than 200 ps peak-to-peak. For comparison we have also included the adjacent 3.5-day data run in Figure 9 with similar information. However, in this series of data the bias-fixed case is only 200 ps peak-to-peak, as is the non-bias-fixed solution.

Figures 10 and 11 show the differences between the bias-fixed and non-bias-fixed solutions for each of the networks separately. In Figure 10 there are several places where the bias-fixed and non-bias-fixed network solutions differ. In Figure 11 the two solutions follow each other closely.

Reviewing the log files for each of these two data series we find that network B had about 30 minutes of missing data at the extra station near PTB, which corresponded to the time of the jump we see shortly after MJD 51596.5 in Figures 8 and 10. There does not however appear to be any outage of station data near the second jump shortly after MJD 51598.

Overlapping data series

Figures 12 and 13 show the differences between adjacent data runs for two different time series of the bias-fixed data. They are the two cases that show the best and worst results over the 48 d analysis period. In Figure 12, the peak-to-peak difference between the half-day merged values is approximately 50 ps. In Figure 13 the peak-to-peak difference is almost 400 ps. This indicates that as we merge the data series we may be making a rate change in the solution whose magnitude might be as large as 5×10^{-15} (worst-case). To determine whether using a different network would make a difference in the solution we plotted an extra network solution, C, in Figure 13. For this network we picked a different station 270 km from PTB, WSRT, that has a hydrogen maser reference. In this case there was a peak-to-peak time difference of 150 ps. This would indicate that maybe the selection of network stations, and possibly their references, might play a part in this rate change as well.

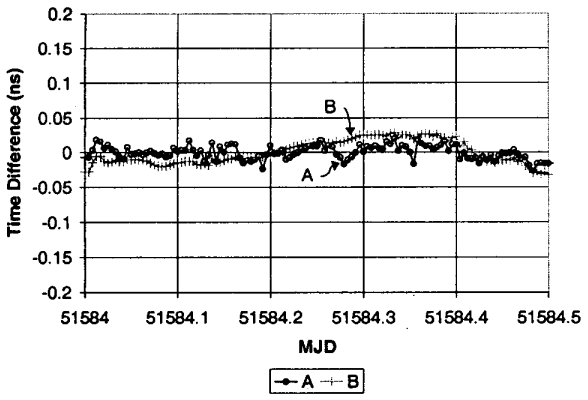

Figure 12: Best-case difference between overlapping values in half-day data merge for Networks A and B from MJD 51584-51584.5.

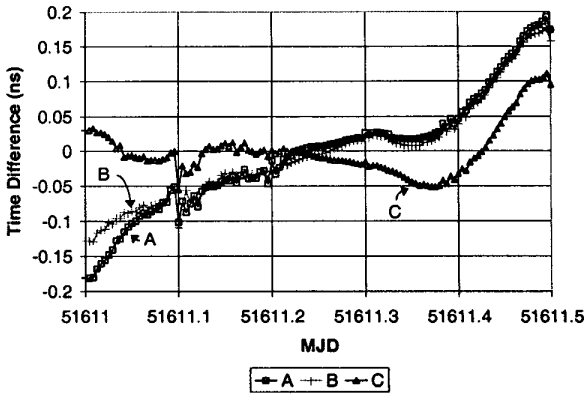

Figure 13: Worst-case difference between overlapping values in half-day data merge for Networks A, B and C, from MJD 51611-51611.5.

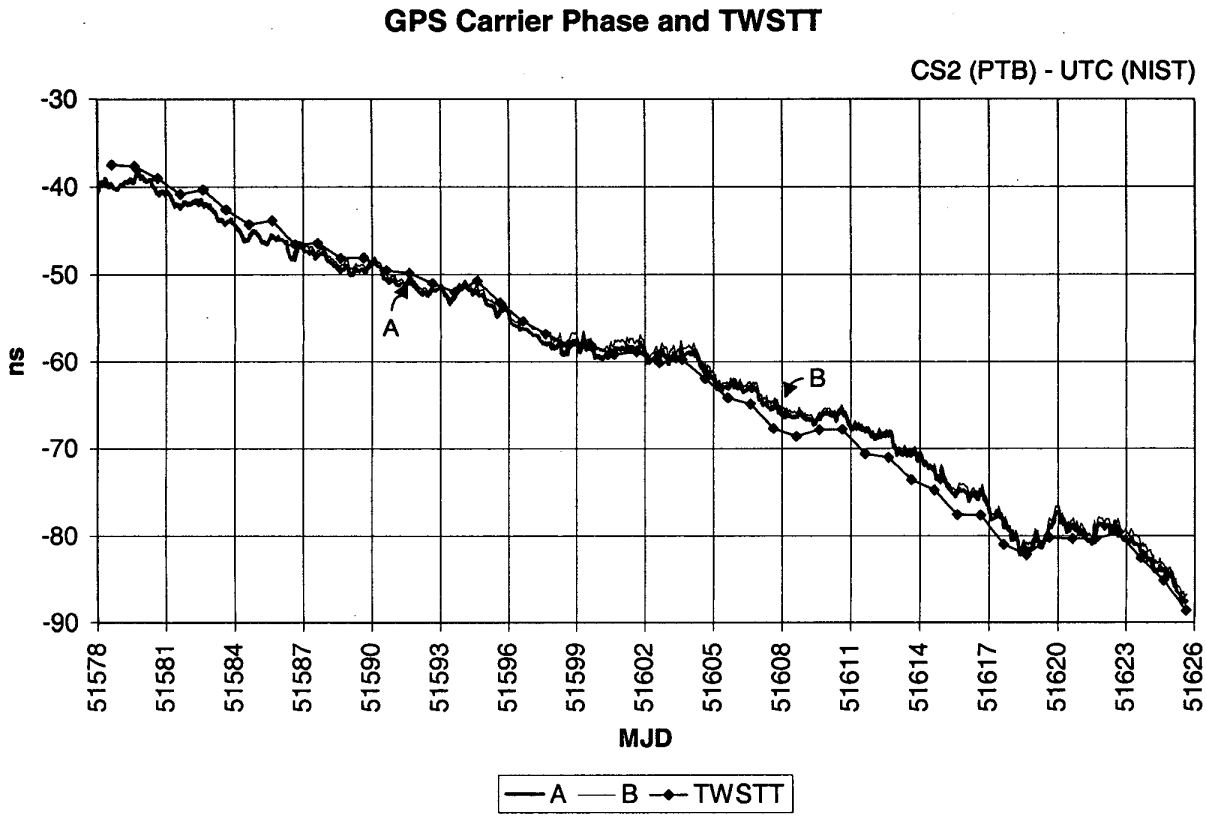

Figure 14: GPS Carrier-phase and TWSTT data for CS2(PTB) – UTC(NIST) from MJD 51578-51626.

CS2 comparison with UTC(NIST)

Figure 14 shows the same data as that of Figure 5, but uses a smoothed hourly correction to transform from H2(PTB) to CS2(PTB) versus UTC(NIST). In this plot we have interpolated the TWSTT to daily points. Once again the carrier-phase and TWSTT results follow each other well in the short term, but there is a slight change in rate over the long term.

Statistics

For statistical purposes we use daily interpolated TWSTT data to compare with our carrier-phase clock estimate solutions. We have also used a 30 d period for our statistical analysis that coincides with the evaluations of the primary frequency standards, NIST-7 and NIST-F1 at NIST. This time period ranges from MJD 51579-51609.

Figure 15 shows the Allan Deviation plot for the H2(PTB) minus UTC(NIST) comparison in Figure 5. At one day both networks A and B are stable to 2.5 parts in 10^{15}, which is the same as the interpolated daily value for the TWSTT data. The Allan Deviation plot for the CS2(PTB) and UTC(NIST) comparison is shown in Figure 16. At one day both Networks A and B are stable to 1.5 parts in 10^{14}, which is the same as the interpolated daily value for the TWSTT data. This figure also includes the Allan Deviation of the CS2(PTB) to H2(PTB) smoothed hourly correction data. The observed noise is fully explainable with the shot-noise limited performance of CS2(PTB), $\sigma_y(\tau = 1\ d) = 1.4 \times 10^{-14}$.

Figure 17 shows the differences between the interpolated TWSTT daily values and daily carrier-phase solutions for each network. At one day we see 3.5 parts in 10^{15} for both differences. For comparison, Figure 18 shows the same difference over the full 48 d comparison interval. In this case the difference is at 4 parts in 10^{15} at one day.

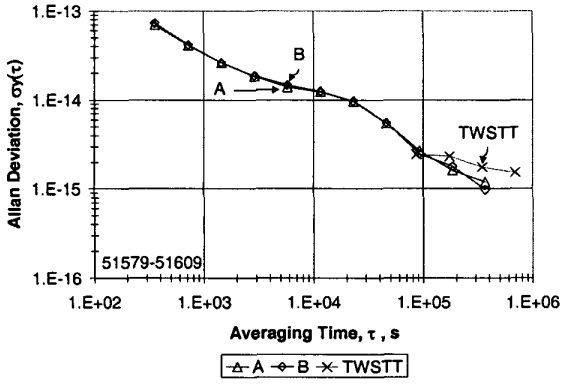

Figure 15: Allan Deviation for H2(PTB)-UTC(NIST) from MJD 51579-51609.

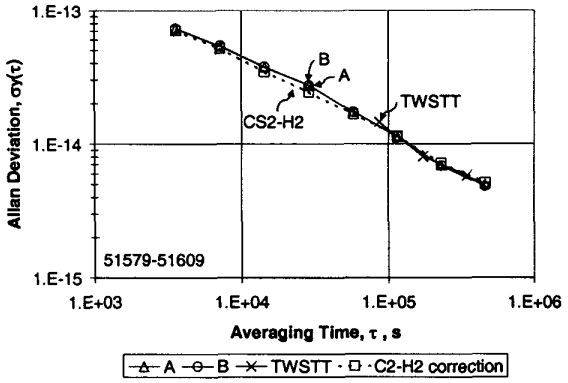

Figure 16: Allan Deviation for CS2(PTB)-UTC(NIST) from MJD 51579-51609.

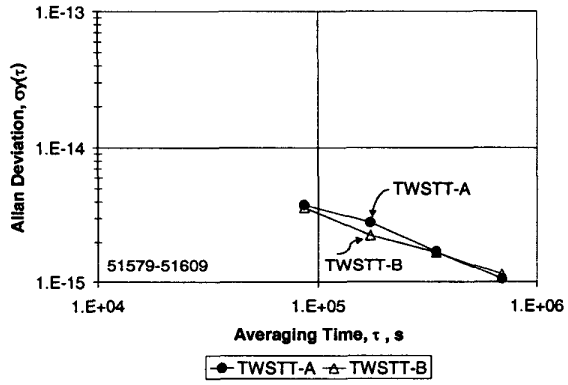

Figure 17: TWSTT-GPS Carrier Phase data for MJD 51579-51609.

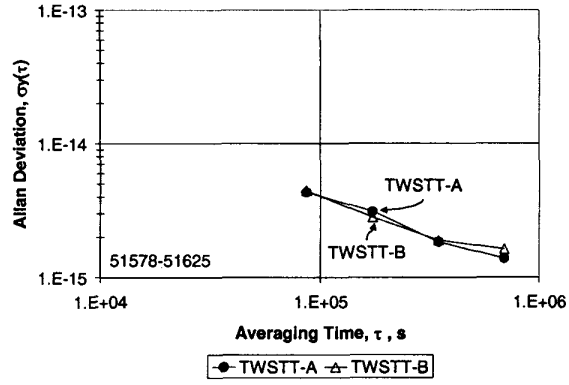

Figure 18: TWSTT-GPS Carrier Phase data for MJD 51578-51625.

Comparison of Atomic Frequency Standards

We also made corrections to the CS2-UTC(NIST) data to compare CS2(PTB) with NIST-F1 and NIST-7. The comparison of the atomic frequency standards is shown in Table 2. The evaluations of the frequency standards at NIST were made between MJD 51579 and 51609. The interval over which values were reported in the Circular T did not exactly match this interval so we made an estimate of the Circular T values over this interval of interest. The Circular T values are GPS common view data results for the NIST-PTB link that are reported on a monthly basis by the BIPM.

We found that the network solutions were both within 2 parts in 10^{15} of the TWSTT and the Circular-T estimates and uncertainties for both the NIST-F1 and NIST-7 comparisons.

Table 2: Comparison of Atomic Frequency Standards at NIST and PTB.

51579-51609	Estimated Circular T	A	B	TWSTT
CS2 – NIST-F1	-2.3E-15	6.94E-16	8.50E-16	-9.82E-16
CS2 – NIST-7	1.7E-15	4.79E-15	4.95E-15	3.12E-15

Conclusions

We will continue to experiment with this link and further investigate the contribution of data gaps, especially due to station outages and how that might be affecting the carrier-phase cycle ambiguity resolution. We also hope to determine the error contribution of data merging into the error budget.

Acknowledgements

The authors thank Dr. Tom Parker and Victor Zhang from NIST for providing data and helpful discussions. We also thank Jürgen Becker from PTB for providing internal data UTC(PTB) - H2(PTB) and CS2(PTB) - H2(PTB).

References

1. Nelson, Lisa, Judah Levine, Kristine Larson, and Peter Hetzel (1999), "Comparison of Atomic Frequency Standards at NIST and PTB using Carrier-phase GPS," to be published in the Proceedings of the 31st Annual Precise Time and Time Interval Applications and Planning Meeting, Dana Pont, CA.

2. Larson, Kristine and Judah Levine (1998), " Time Transfer using the Phase of the GPS Carrier," *IEEE Trans. On Ultrasonics, Ferroelectrics and Frequency Control*, Vol. 45, No. 3, pp. 439-540.

3. Larson, Kristine and Judah Levine (1999), "Carrier-Phase Time Transfer," *IEEE Trans. On Ultrasonics, Ferroelectrics and Frequency Control*, Vol. 46, No. 3, pp. 1001-1012.

4. Larson, Kristine, Lisa Nelson, Judah Levine, Thomas Parker and Edward Powers (1998), "A Long-term Comparison between GPS Carrier-Phase and Two-Way Satellite Time-Transfer," Proc. 30th Annual Precise Time and Time Interval Applications and Planning Meeting, Reston, VA, pp. 247-255.

5. Larson, Kristine M., Judah Levine, Lisa M. Nelson, and Thomas E. Parker (2000), " Assessment of GPS Carrier-Phase Stability for Time-Transfer Applications," *IEEE Trans. On Ultrasonics, Ferroelectrics and Frequency Control*, Vol. 47, No. 2, pp. 484-494.

6. Lichten, S. and J. Border (1987), " Strategies for High-Precision Global Positioning System Orbit Determination", *Journal of Geophysical Research*, 92, pp. 12,751-12,762.

7. Beutler, G., I. I. Mueller, and R. E. Neilan (1994), "The International GPS Service for Geodynamics (IGS): Development and start of official service on January 1, 1994," Bulletin Geodesique, 68(1), pp. 39-70.